TSUNAMI RUN-UP MODEL AND INUNDATION MAPS FOR MALAYSIA

TAN WAI KIAT

UNIVERSITI SAINS MALAYSIA

2017

TSUNAMI RUN-UP MODEL AND INUNDATION MAPS FOR MALAYSIA

by

TAN WAI KIAT

Thesis submitted in fulfillment of the requirements for the degree of Doctor of Philosophy

August 2017

ACKNOWLEDGEMENT

I would like to thank all the people who contributed in some way to the research described in this thesis. First and foremost, I would like to convey my heartfelt gratitude to my supervisor, Associate Professor Dr Teh Su Yean, for accepting me as a PhD student. During my studies, she contributed to a rewarding graduate school experience by giving me intellectual freedom in my research, supporting my participation in various conferences and workshops, engaging me in new ideas and demanding a high quality of work in all my endeavors. In addition, she has showed me how to dissect life challenges into many different ways and to look at them from different angles, grooming me into a better individual. This thesis would not have been possible without her extraordinary support. My warmest thanks also go to my field supervisor, Prof Koh Hock Lye, I deeply appreciate his constant support, availability and constructive suggestions. It is a great pleasure and honor to work under his supervision. Again, this thesis would not be completed without the contributions of Dr Teh and Prof Koh. Therefore, I am thankful to them from the bottom of my heart. I would like to thank the Science Fund Grant #305/PMATHS/613418 from Ministry of Science, Technology and Innovation (MOSTI) for supporting me during this entire research duration. Besides that, I am also very grateful to be a recipient of MyPhD scholarship under the MyBrain15 program from the Ministry of Higher Education (MOHE). Moreover, the high-resolution bathymetric and topographic data provided by Pusat Hidrografi Nasional (PHN) and Jabatan Ukur dan Pemetaan Malaysia (JUPEM) respectively are also acknowledged. In October 2014 and May 2015, I was offered fellowships to participate in high-performance computing workshops in the International Center of Theoretical Physics (ICTP) located in Trieste, Italy. I am greatly indebted for the

excellent academic environment that is inspiring. In addition, in May 2016, I was also offered a fellowship to participate in a wave modeling workshop in Institut Teknologi Bandung (ITB) located in Bandung, Indonesia. It is an honor for me to be given such opportunity to explore the research environment in one of the most prestigious research institution in Indonesia. I take this opportunity to thank the School of Mathematical Sciences (PPSM) and Institute of Postgraduate Studies (IPS), Universiti Sains Malaysia (USM) for the generous provision of facilities and space to the completion of this thesis. I also wish to tender my appreciation to my colleagues in USM, Kh'ng Xin Yi and Lim Yong Hui, for assisting me in my research. To my close friends, I express my gratitude for their unconditional friendship, support and patience throughout these years. Finally, my deepest gratitude goes to my family for their unflagging love and support throughout my life, and without which I would not have come this far.

TABLE OF CONTENTS

LIST OF TABLES

LIST OF FIGURES

LIST OF SYMBOLS

$\|\|$	Chinnery's notation
A	maximum wave height of a solitary wave
a_0	initial acceleration
b	total length of a slide
C_d	drag coefficient
C_m	added mass coefficient
C_n	Coulomb friction coefficient
d	water depth
D	initial submergence depth
$\mathbf{D}$	Burger's vector
D_I	inundation distance
$d_{\max}$	maximum water depth
g	gravitational acceleration constant
h	total water depth
H	height-to-depth ratio
$H_{\min}$	minimum threshold depth
h_{node}	total water depth at a node
i, j	finite difference spatial node
I_{depth}	inundated depth
k	finite difference temporal node
L	length of a fault plane
$l/2$	half wavelength
M_w	Richter scale
n	Manning's roughness coefficient

R	run-up height
$s(t)$	center of mass motion
s_0	characteristic distance of motion
t	time
T	maximum thickness in the center of a slide
t_0	characteristic time of motion
U	flux in the x-direction
u_t	theoretical terminal velocity
V	flux in the y-direction
W	width of a fault plane
w	width of a slide
x, y	horizontal distance
x_0	location at the toe of a slope
x_c, y_c	center of a solitary wave with maximum wave height
$X_{\min}$	position of the maximum depression
$Z_{\max}$	maximum elevation of a submarine landslide-generated tsunami
$Z_{\min}$	maximum depression of a submarine landslide-generated tsunami
α	coefficients of upwind scheme
γ	wave number
δ	dip angle
Δt	time step
$\Delta x, \Delta y$	spatial grid size
Δx_m	distance between the maximum depression and maximum elevation
η	vertical free surface displacement
η_0	two-dimensional characteristic tsunami amplitude

θ	angle of a planar slope
κ	slip angle
λ_0	characteristic wavelength
v	angle between **D** and the fault plane
π	pi
ρ	specific density
φ	strike angle

LIST OF ABBREVIATIONS

1D	one-dimensional
2D	two-dimensional
3D	three-dimensional
ANUGA	Australian National University-Geoscience Australia
COMCOT	Cornell Multi-grid Coupled Tsunami
COULWAVE	Cornell University Long and Intermediate Wave Modeling Package
DSWG	Directional Spectral Wave Generator
FD	finite difference
FV	finite volume
FVCOM	Finite Volume Coastal Ocean Model
GEJET	Great Eastern Japan Earthquake and Tsunami
GIS	geographic information system
GPS	global positioning system
HPC	high-performance computing
ISEC	Inundation Science & Engineering Cooperative
JUPEM	Department of Survey and Mapping Malaysia
MBA	moving boundary algorithm
MOST	Method of Splitting Tsunami
MSL	mean sea level
NHWAVE	Non-Hydrostatic Wave
NOAA	National Oceanic and Atmospheric
NSCS	Northern South China Sea
NSWE	nonlinear shallow water equations

NTHMP	National Tsunami Hazard Mitigation Program
NWBT	Northwest Borneo Trough
PHN	National Hydrographic Center
PNG	Papua New Guinea
POM	Princeton Ocean Model
QGIS	Quantum Geographic Information System
SCS	South China Sea
SMF	submarine mass failure
SW	shallow water
TUNA	Tsunami-tracking Utilities and Application
TUNA-LS	Tsunami-tracking Utilities and Application: Landslide
TUNAMI-N2	Tohoku University's Numerical Analysis Model for Investigation of Near-field tsunamis, No. 2
TUNA-RP	Tsunami-tracking Utilities and Application: Run-up
WD	wetting-drying

MODEL RAYAPAN TSUNAMI DAN PETA INUNDASI

UNTUK MALAYSIA

ABSTRAK

Penyelidikan ini bertujuan untuk menilai kerentanan persisiran pantai Malaysia terhadap tsunami yang berasal dari zon subduksi berdekatan, iaitu Peparit Sunda and Peparit Manila, dan dari Longsoran Brunei. Bagi tujuan ini, satu model rayapan tsunami dua dimensi, dengan nama kod TUNA-RP, telah dibangunkan dan disahkan dengan satu set masalah penanda aras piawai. Simulasi model dijalankan untuk menghasilkan peta inundasi bagi persisiran pantai Malaysia yang terjejas oleh tsunami yang berasal dari Peparit Sunda, Peparit Manila dan Longsoran Brunei. Peta inundasi sering digunakan oleh pihak berkuasa dan masyarakat tempatan sebagai asas untuk merancang laluan evakuasi dan mengurus pembangunan di persisiran pantai. Untuk menguji kemantapan TUNA-RP, peta inundasi Langkawi, Kedah dan Pulau Pinang yang dihasilkan adalah sepadan dengan data lapangan Tsunami Lautan Hindi 2004. Penemuan penting dilaporkan seperti berikut. Pertama, keputusan simulasi menunjukkan gelombang tsunami yang dijana oleh Peparit Manila tidak menimbulkan ancaman serius kepada Kudat, Kota Kinabalu dan Labuan. Namun, bandar Miri dan Bintulu di Sarawak terdedah kepada risiko yang lebih tinggi daripada tsunami yang berasal dari Peparit Manila. Oleh itu, keperluan untuk program daya tahan dan kesiapsiagaan masyarakat di lokasi ini perlu dititikberatkan. Kedua, kegagalan jisim bawah laut (SMF) yang besar boleh menghasilkan tsunami dengan impak yang lebih buruk berbanding tsunami yang dijana oleh pergerakan menegak dasar laut yang berasal daripada aktiviti tektonik, juga dikenali sebagai tsunami gempa bumi. Hal ini kerana SMF sering berlaku di

batasan berhampiran persisiran pantai, ia tidak boleh diramal dengan tepat, dan boleh tiba dalam masa beberapa minit selepas longsoran. Ketiga, keputusan simulasi menunjukkan bahawa dalam senario yang paling teruk, tsunami yang dijana oleh SMF di luar Brunei boleh melanda persisiran pantai Sabah dengan tinggi gelombang yang besar dalam masa lebih kurang dari sejam. Kudat, Kota Kinabalu, Labuan dan Miri diramal akan teruk dibanjiri, dengan kedalaman inundasi berpotensi mencapai 20 m pada beberapa kawasan. Gelombang tsunami boleh membanjiri pantai rendah di Miri sehingga 4.86 km. Oleh itu, adalah penting untuk membangunkan langkah-langkah mitigasi tsunami dan memupuk daya tahan masyarakat di sepanjang pantai yang terjejas di Sabah dan Sarawak yang dikenal pasti dalam penyelidikan ini supaya impak buruk tsunami dapat dikurangkan.

TSUNAMI RUN-UP MODEL AND INUNDATION MAPS FOR MALAYSIA

ABSTRACT

This study mainly aims to assess the vulnerability of Malaysian coasts to tsunamis originating from nearby subduction zones, namely the Sunda Trench and the Manila Trench, and from the Brunei Slide. For this purpose, a two-dimensional tsunami run-up model, codenamed TUNA-RP, is developed and validated against a standard set of benchmark problems. Model simulations are performed to produce the inundation maps for the affected Malaysian coasts for tsunamis originating from the Sunda Trench, the Manila Trench and the Brunei Slide. Inundation maps often serve as the basis for authorities and local communities to plan evacuation route and manage coastal development. Intended to test the robustness of TUNA-RP, the inundation maps produced for Langkawi, Kedah and Penang match well with the measured field data compiled from the 2004 Indian Ocean Tsunami. Significant findings are reported as follows. First, the simulation results show that the tsunami wave generated by the Manila Trench does not pose serious threats to Kudat, Kota Kinabalu and Labuan. But the towns of Miri and Bintulu in Sarawak appear to be exposed to higher risk from tsunami originating from the Manila Trench. This highlights the need for community resilience and preparedness program at these locations. Second, large Submarine Mass Failure (SMF) can indeed generate tsunamis with more disastrous impact than tsunamis generated by vertical uplift of sea-bottom from tectonic activity, known as earthquake-generated tsunami. This is because SMF often occurs on coastal margins near shorelines, cannot be predicted with accuracy, and may strike within minutes following mass failure. Third,

simulation results indicate that under the worst case scenario, the tsunami generated by SMF off Brunei, could strike the coast of Sabah with large wave heights reaching coastal cities in less than an hour. Kudat, Kota Kinabalu, Labuan and Miri are projected to be badly inundated by the tsunami waves, with inundated depth at some locations potentially reaching 20 m. The tsunami waves can inundate the low-lying coasts of Miri for up to 4.86 km inland. Hence, it is important to develop tsunami mitigation measures and to cultivate community resilience along the affected coasts of Sabah and Sarawak identified in this research in order to reduce the adverse impacts.

CHAPTER 1

INTRODUCTION

1.1 Introduction to Tsunami

A tsunami is an oceanic gravity long wave generated by submarine or other coastal geological processes such as earthquakes, landslides or volcanic eruptions. Most tsunamis are generated by large shallow earthquakes along subduction zones of tectonic plates. They usually propagate across deep ocean with long wavelengths and small wave heights, and hence are difficult to be noticed. However, the wavelengths are shortened and wave heights are amplified as the tsunami waves enter continental shelf where the water depths are shallow, as illustrated in Figure 1.1. This in turn may cause devastating destructions when the tsunami waves arrive at low-lying beaches or harbors.

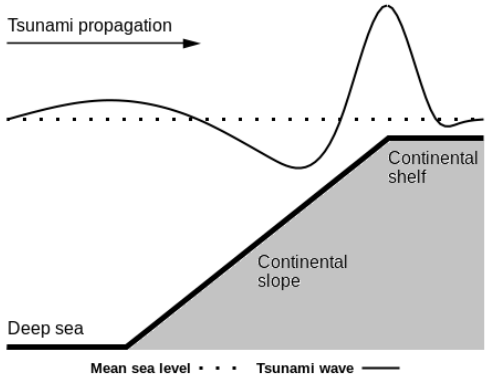

Figure 1.1: Amplification of wave height as tsunamis enter continental shelf

An earthquake of Richter scale M_w = 9.3 occurred off the Sumatra Island, Indonesia on 26 December 2004, generating a tsunami that devastated the coasts of neighboring countries in the Indian Ocean. The tsunami killed around 250,000

people in the affected areas. Without a good understanding of tsunami hazards in the region, Malaysians mistakenly perceived its coasts as safe from tsunami risks, and suffered a loss of 68 deaths. Seven years later, on 11 March 2011, an earthquake of magnitude M_w = 9.0 occurred off the Pacific coast of Tohoku, Japan. This earthquake generated a violent tsunami that claimed 20,000 casualties and destroyed many coastal settlements and infrastructures including the Daiichi Nuclear Power Plants. These two devastating tsunamis in the recent past prompted many to pay attention to the risks posed by tsunamis, to develop tsunami mitigation measures and to cultivate tsunami resilience among the local coastal communities. This thesis is an integral part of the concerted efforts towards making Malaysian coastal communities more resilient to the impacts of tsunamis.

1.2 Tsunami Run-up and Inundation

Experts from different background, such as mathematics, coastal engineering and geology, and from different countries often form international tsunami survey teams to conduct immediate post-tsunami site surveys for documenting tsunami impacts. An essential component of the surveys is to measure the inundation distance and run-up height along the coast. As displayed in Figure 1.2, inundation distance D_I is defined as the horizontal distance of wave penetration measured from the nearest landward mean sea level (MSL); and run-up height R is defined as the maximum vertical height of wave uprush measured above MSL. In addition, inundated depth I_{depth} is the water depth on dry land measured above ground surface. These definitions will be used frequently throughout this thesis.

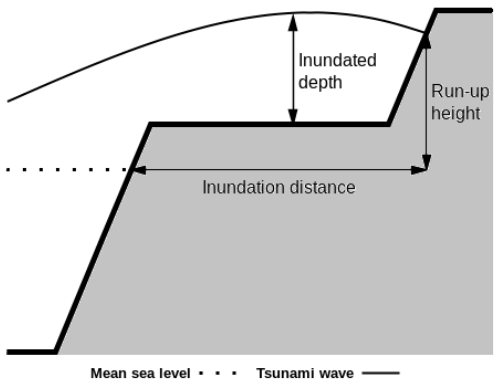

Figure 1.2: Definitions of inundation distance, run-up height and inundated depth

Field surveys are usually conducted at the earliest time after the rescue efforts. The inundation limits are first identified based on the tsunami traces, such as watermarks left on building walls, saltwater discolorations or lines of debris deposited on beaches. The approximate inundation distances are then estimated perpendicular to the shoreline and the respective run-up heights are measured using portable Global Positioning System (GPS) measurement instruments (Goto et al., 2012). If there is a lack of physical evidence, the run-up heights are estimated based on interviews with eyewitnesses, but are considered less reliable.

Immediately after the 2004 Indian Ocean tsunami event, many scientists from all over the world visited the affected coasts to document the tsunami impacts. The measured run-up heights in the Sumatra Island, particularly in the Aceh province, were mostly higher than 20 m with the maximum of 32 m (Borrero, 2005). The run-up heights along the Andaman Sea coast were highly variable, from 5 to 15 m in Thailand (Tsuji et al., 2006), less than 3 m in Myanmar (Imamura et al., 2006) and less than 4 m in Malaysia (Koh et al., 2009). In the aftermath of the 2011 Great Eastern Japan Earthquake and Tsunami (GEJET), site surveys revealed that run-up height of the tsunami was spatially variable, ranging from 3 m to 35 m (Lin et al.,

2012). Large run-up heights were recorded mainly in the areas which are close to the epicenter of earthquake. Recently, a magnitude of M_w = 6.9 earthquake occurred off Honshu Island in Japan on 22 November 2016 at 5:59 a.m. local time, generating tsunami waves in the coast of Fukushima. This quake struck close to the epicenter of the 2011 and brought back traumatic memories for the locals of the devastating 2011 GEJET. Tsunami warnings were issued quickly for east coast of Fukushima, urging the local to immediately seek higher ground. The wave heights of 1.4 m and 1.0 m are recorded at Sendai port and Fukushima nuclear plant respectively. Documentation of past tsunami events serves as guidelines to better prepare the coastal communities for future potential tsunamis.

1.3 Tsunami Modeling

Tsunami modeling is widely utilized to simulate a complete cycle of tsunami dynamic, which consists of generation, propagation and inundation, for simulating the tsunami wave height, arrival time, inundation distance and run-up height. These simulated projections are in turn used to aid the tsunami hazard authorities and local communities to plan and implement evacuation and mitigation measures.

The key to modeling earthquake-generated tsunami is to understand the transfer of kinetic energy from vertical displacement of seabed to sea surface waves. Because of the mathematical simplicity, the Okada model based on a homogeneous half-space assumption is the most widely applied model in projecting the initial sea surface displacement generated by an earthquake. However, modeling submarine landslide-generated tsunami is more complicated for various reasons, such as the

coupling between fluid and solid motions, the lack of real event data and the involvement of more physical parameters.

The tsunami propagation speed depends on the water depth which is not uniform across the ocean. Various simulation models are developed based upon linear shallow water equations to study the tsunami propagation. Realistic or actual bathymetry data can be incorporated into these simulations model to accurately project arrival time of tsunamis. However, the modeling of tsunami run-up and inundation continue to be a challenging problem despite it having been intensively studied during the last sixty years. This is because the governing equations, such as the nonlinear shallow water equations, the Navier-Stokes equations and the Boussinesq equations, are valid only if there is a positive water depth, i.e. these governing equations are not applicable on dry land where water depth is zero. Therefore, an appropriate wetting-drying (WD) algorithm is necessary to be incorporated into the governing equations to solve this problem. In addition, high resolution topographic and bathymetric data are required to accurately model the tsunami run-up and inundation. This in turn increases the size of computational domain and pose another challenge.

1.4 Objectives of Thesis

The objectives of this thesis are as follows:

1. To develop a tsunami run-up and inundation model, codenamed Tsunami-tracking Utilities and Application-Runup (TUNA-RP);
2. To develop a submarine landslide tsunami generation model, codenamed Tsunami-tracking Utilities and Application-Landslide (TUNA-LS);

3. To produce inundation maps for Malaysia via TUNA-RP simulations of future potential tsunami sources, including the Manila Trench and the Brunei Slide.

1.5 Scope and Organization of Thesis

This thesis begins with a brief introduction to tsunami and its impacts on coastal communities, drawing insights from two past mega tsunami events such as the 2004 Indian Ocean tsunami and the 2011 GEJET. The need of incorporating tsunami modeling in tsunami hazard assessment is highlighted and the challenges of tsunami modeling are then explored, leading to the focus of this thesis. This is followed by the objectives, scope and organization of this thesis.

Chapter 2 presents a review of related literature, beginning with earthquake-generated and submarine-landslide generated tsunamis as well as research related to these events. The 2011 GEJET is then specially reviewed because of the recorded run-up heights were highly spatially variable, reaching 40 m in some locations. Intensive studies have led to the hypothesis that the GEJET is a combination of an earthquake-generated tsunami and a submarine landslide generated tsunami. This is followed by a discussion on inundation maps as an essential element of tsunami hazard assessment. A review of the tsunami run-up and inundation models is presented and this leads to the discussion of four WD algorithms: (i) thin film, (ii) element removal, (iii) extrapolation and (iv) negative depth and finally the choice of a specific WD algorithm to be implemented into TUNA-RP.

Detailed discussions on the nonlinear shallow water equations and the moving boundary algorithm form the focus for Chapter 3, which stimulates the interest in developing an in-house two-dimensional tsunami run-up model, codenamed TUNA-RP. TUNA-RP is then validated via a standard set of benchmark problems. Satisfactory comparisons between the simulated results and these benchmark data are then presented. Finally, calibration of TUNA-RP to study the sensitivity analysis of run-up height to minimum threshold depth and Manning's roughness coefficient is presented to round-up this chapter.

The introduction to the Okada model, a commonly applied earthquake tsunami generation model, will first be presented in Chapter 4. This leads to the hindcasting of TUNA-RP via the 2004 Indian Ocean tsunami simulation. The simulated run-up heights are then compared to the survey data to verify the capability of TUNA-RP in producing practical inundation maps. The inundation maps are produced by overlaying TUNA-RP simulation results onto Google Earth maps using Quantum Geographic Information System (typically referred to as QGIS) is then discussed. In the final section of this chapter, the potential tsunami risk generated by the deformation of the Manila Trench is assessed via TUNA-RP simulation.

Submarine landslide-generated tsunamis are known to have caused more disastrous impacts if compared to earthquake-generated tsunamis generated by displacement of similar size. The potential submarine landslide-generated tsunami by the Brunei Slide located at the continental slope of Baram Canyon is the focus of Chapter 5. A submarine landslide tsunami generation model, codenamed TUNA-LS, is developed for projecting the initial tsunami wave caused by the submarine Brunei

Slide. The simulated initial tsunami wave is then utilized as the initial condition for propagation simulations, the simulation results of which are in turn utilized for TUNA-RP simulation to produce inundation maps.

This thesis ends with a summary regarding future research direction and improvement on tsunami modeling in Chapter 6.

CHAPTER 2

LITERATURE REVIEW

Tsunamis are rare but potentially catastrophic events that pose real hazards to many coastal communities worldwide. The 2011 Great Eastern Japan Earthquake and Tsunami (GEJET) is a grim reminder of the unpredictability of nature. Believed to have the most advanced tsunami warning system Japan, nevertheless, was not ready for the devastating impact brought upon by GEJET. Scientists now believe that no subduction zone is safe from a megaquake; and that a fault does not necessarily produce earthquakes of the same size, nor with the same regularity every time a quake occurs. Malaysia was mistakenly perceived as safe from tsunami hazards until the 2004 Indian Ocean tsunami. Since the event, Malaysia has begun active research on tsunami to prepare coastal community to mitigate future potential tsunamis. Reviews on past tsunami events are essential for researchers to understand the generation, dynamics and impact of tsunamis. In this review chapter, the past events of earthquake-generated and submarine landslide-generated tsunamis as well as research related to these events are first presented. This is followed by a review of the tsunami run-up and inundation models, which leads to the discussion about various WD algorithms used and finally the choice of a specific WD algorithm to be implemented into TUNA-RP.

2.1 Earthquake-Generated Tsunamis

Earthquake generated tsunamis are common occurrences in certain parts of the world. In the Far East of Russia, especially in the Kamchatka Peninsula and the Kurile Islands, tsunami run-up heights reaching 15 m to 20 m or higher have been

repeatedly observed for the past 250 years. The tsunami catalogue of the Russian Far East from 1737 to the present lists 110 events that document several characteristics regarding tsunami occurrence. Most tsunamis in the Russian Far East are near-field (105 events) with a few far-field (5 events) sources. Altogether, there were eleven devastating tsunamis, with more than 10 m wave heights, two of which were mega events with tsunami waves exceeding 20 m in 1737 and 1952. The average recurrence period for tsunamis of different magnitudes in the Russian Pacific coast is 25 years for devastating events and 10 to 15 years for hazardous tsunamis, with wave heights in the rage of 2.5 to 10 m. Note that, small tsunamis occur almost every year. Most of the catalogued tsunamis were induced by earthquakes, occurring 95 times (Gusiakov, 2016). This Russian catalogue provides a glimpse to occurrence frequency of earthquake-generated tsunami. In this section, three large tsunamis in the recent past are reviewed and the simulation models used in each tsunami event are discussed.

2.1.1 The Chile Tsunami on 22 May 1960

The largest earthquake of magnitude M_w = 9.5 in the twentieth century occurred offshore of southern Chile on 22 May 1960, generating a devastating tsunami that severely damaged the Chilean coast and caused more than 1000 deaths. This tsunami then propagated across the Pacific Ocean, arriving at the Hawaiian Islands after 15 hours later and at the Japanese Islands after 23 hours. Wave heights of 2 m and 5 m were recorded in Hawaii (Liu et al., 1995b) and Japan (Satake, 2002) respectively. Although Japan is located further away from the source location, the bathymetry in the Pacific Ocean focuses the wave energy towards the Japanese

Islands (Shuto, 1991). Therefore, Japan received higher wave heights during this disastrous tsunami event if compared to those in Hawaii.

To simulate the transoceanic propagation of this 1960 Chilean tsunami across the Pacific Ocean and ultimately the local run-up and inundation in Hawaii, Liu et al. (1995b) employed the Cornell Multi-Grid Coupled Tsunami (COMCOT) model. COMCOT solves the linear shallow water equations in the propagation simulation and solve the nonlinear shallow water equations (NSWE) with a moving boundary algorithm (MBA) in the run-up and inundation simulation. An explicit leapfrog finite difference scheme is used in both simulations. The simulated arrival times of tsunami wave in Hawaii compared well to the observed data. However, the COMCOT model over-simulated the maximum inundation distance with an over estimation of approximately 200 m, because a large grid size of 100 m was used in the inundation simulation. The choice of 100 m large grid size was adopted due to insufficient computational resources. It should be noted that the inundation simulation results can be improved if a finer spatial grid size is used.

2.1.2 The Okushiri Tsunami on 12 July 1993

Japan has a long history of experiencing tsunamis. On 12 July 1993, a tsunami was generated by the Southwest Hokkaido earthquake of magnitude M_w = 7.8. Okushiri Island, a pear-shaped island located within the earthquake source region, was hit by the tsunami within minutes with an unexpectedly high measured run-up height of 20 m at the lee side of the island (Takahashi et al., 1995). This unexpected phenomenon became one of the best-studied event for tsunami modeling research community to understand the wave wrap-around effect that can vastly amplify wave

heights. Titov and Synolakis (1997) utilized a simulation model based on the non-conservative NSWE to simulate this 1993 Hokkaido tsunami event, focusing on the distribution of run-up heights on the Okushiri Island. The model employs the finite difference scheme to solve the NSWE and the depth extrapolation algorithm to simulate run-up and inundation on dry land. Simulated run-up heights were generally higher than the measured data because the simulation did not include wave dissipation. Titov and Synolakis (1997) also noted that fine resolution of bathymetric data at coastal region is important in proper inundation simulation, as is commonly observed. Overall, the NSWE models with fine grids have been proven to be adequate for modeling the high run-up at the lee side of the Okushiri Island caused by the wave wrap-around effect.

2.1.3 The Indian Ocean Tsunami on 26 December 2004

The great earthquake of magnitude M_w = 9.3 that occurred off the Sumatra Island, Indonesia on 26 December 2004 generated a series of tsunami waves that affected more than ten countries around the Indian Ocean, including Indonesia, Sri Lanka, Thailand, Malaysia. This mega-tsunami resulted in a death toll of around 250,000 and caused great economic losses. The whole world was heavily shocked by this devastating natural disaster.

The tsunami propagated in two distinct directions towards the east and the west, due to the wave directivity of energy. The tsunami waves travelled east towards the coasts of Thailand and Malaysia, located approximately 500 km away, after passing through the Andaman Sea. Another tsunami wave travelled toward the west, propagating across the Indian Ocean and arriving at the coasts of India and Sri

Lanka. The water depth in the Andaman Sea is shallower, at 500 m to 600 m, compared to the water depth in the Indian Ocean, at 4000 m to 5000 m (Imamura, 2008). Hence the waves travelled slower through the Andaman Sea. In addition, the tsunami wave propagated toward Thailand and Malaysia was a leading-depression N-wave, while the tsunami wave propagated toward India and Sri Lanka was a leading-elevation N-wave.

After the 2004 Indian Ocean tsunami event, rigorous tsunami modeling research had been carried out worldwide to better understand the impacts of this transoceanic tsunami. Borrero et al. (2006) simulated the 2004 tsunami using the Method of Splitting Tsunami (MOST), a well-known operational tsunami model, for assessing the extent of inundation in western Sumatra. MOST solves the NSWE with a finite difference scheme coupled with a depth extrapolation algorithm to simulate run-up on dry land. Koh et al. (2009) successfully utilized an in-house tsunami simulation model, codenamed TUNA, to simulate the wave heights and arrival times at several offshore locations around Malaysia. Teh et al. (2009) simulated the passage of the tsunami waves over mangrove forests and suggested the preservation of mangrove forests as a bio-shield to reduce tsunami impacts. Mishra et al. (2014) evaluated the tsunami vulnerability along the northeast coast of India using the Tohoku University's Numerical Analysis Model for Investigation of Near-field tsunamis, No. 2 (TUNAMI-N2). Similar to MOST, TUNAMI-N2 also solves the NSWE with a finite difference scheme, but employs an element removal algorithm to simulate run-up on dry land. Tsunami simulations have been extensively used as an integral component in tsunami hazard assessment, in tsunami impact mitigations and in tsunami awareness and educating for affected coastal community.

2.2 Submarine Landslide-Generated Tsunamis

Submarine landslide or submarine mass failure (SMF) with mass volume of 1 km^3 or more can potentially generate very destructive tsunamis that can cause extensive damage to seafloor infrastructures (Pope et al., 2015). SMF can generate tsunami with amplitude that far exceeds that generated by co-seismic uplift of seafloor of similar volume. Tsunamis generated by SMF is a potential major coastal hazards even for moderate earthquakes of magnitude M_w = 5.5 and above that occur in or near the coasts (Tappin et al., 2001). Large SMFs are often triggered on the continental slope, because such a landslide's vertical downward movement may reach several thousand meters. The large potential energy is then transferred to large kinetic energy, generating large tsunamis that leave little time for preparation or evacuation since the tsunami occurs near the coastal region. For example, in 1946, a magnitude M_w = 7.1 earthquake triggered a giant (≈ 200 km^3) submarine landslide along the Aleutian Trench, generating the giant Unimak, Alaska tsunami (Fryer et al., 2004). The landslide mass was located within the shallow continental shelf in 150 m water depth, and the landslide mass moved down at a 4° slope to the 4000 m deep Aleutian Trench. Recorded run-up height for this massive tsunami event reached 35 m above mean sea level at the Scotch Cap lighthouse (Lander, 1996). SMFs are major natural marine disasters that could critically damage coastal facilities such as nuclear power plants, as seen during the 2011 Fukushima dual earthquake-generated and landslide-generated tsunami. SMFs can endanger deep-water oil and gas exploration and development platforms, as well as damage pipelines, submarine cables and other submarine facilities. A major concern for the oil and gas industry in Malaysia is therefore the potential of violent earthquakes west of the Philippines, or of strong volcanoes at the Sunda Straits of Indonesia and

large submarine landslides in the South China Sea. With ongoing active development of offshore industry in East Malaysia (Sabah and Sarawak), it is essential to investigate SMFs, for potential tsunamis hazard assessment, as SMFs are common. In a study to assess tsunami hazard in the U.S. East Coast using relationships between submarine landslides and earthquakes, Brink et al. (2009) concluded that the calculated areas of slope failure at some locations are sufficiently large for earthquakes with magnitude greater than M_w = 5.5 to cause a devastating tsunami if the epicenter is optimally located at the base of the upper slope and if the entire area indeed fails. This research finding has immediate implication to potential SMF in the North West Borneo Trough, sharing similar characteristics. A brief account of some other SMFs is provided in the following three subsections, followed by a brief description of SMF-generated tsunami models.

2.2.1 The Ritter Island, Papua New Guinea Tsunami on 13 March 1888

The 13 March 1888 lateral collapse of the Ritter Island of Papua New Guinea (PNG) into the ocean is the largest volcano lateral collapse recorded. The collapse that occurred around 6:00 a.m. removed most of the island. This collapse of the volcano was preceded by explosions accompanied by earthquakes. It produced a large, regionally destructive tsunami that was witnessed by literate observers who timed the waves with watches and provided detailed accounts. That data has been the key to modelling the generation of the tsunami by the landslide and its subsequent propagation (Ward and Day, 2003). Understanding how submarine landslides from volcano collapses generate these tsunamis is important. The deposits of the debris avalanche left by the collapse have been mapped and described by using full-coverage multibeam bathymetry, side-scan sonar backscatter intensity mapping, by

chirp seismic-reflection profiles, TowCam photographs of the seafloor and samples from a single dredge (Day et al., 2015). The Ritter landslide deposits show three distinct morphological facies: (a) initial large block debris avalanche, (b) matrix-rich debris avalanche and (c) distal debris flow facies. A volume of 4.2 km^3 is estimated for the initial collapse. The matrix-rich facies volume is unknown, but large scale erosion of the marine sediment substrate yielded a minimum total volume of 6.4 km^3 in the distal debris flow and turbiditic deposits, highlighting the efficiency of substrate erosion during the later evolution of the landslide movement (Day et al., 2015).

2.2.2 The Papua New Guinea Tsunami on 17 July 1998

The PNG tsunami struck on 17 July 1998, devastating three villages and causing the loss of over 2200 lives. The knowledge that this devastating tsunami was triggered by a moderate earthquake (M_w = 7.0) caught the scientific community attention. Subsequent intensive research suggests that coastal areas with large sediment deposits (such as the Northwest Borneo Trough) are at significant risk from potential SMF. Since then the potential hazards from tsunamis generated by SMF is duly recognized, leading to active research in this field. Before the PNG tsunami, it was questionable as to whether SMFs could really cause devastating tsunamis (Heinrich et al., 2001). Because of this ambiguity concerning the potential impact of SMF, modeling of SMFs as tsunami sources had not been actively pursued up to then. The occurrence of SMF-induced PNG tsunami in 1998 instigated a major scientific investigation in the sea area, offshore of the devastated coastline, with five focused, large-scale, international programs of marine surveying taking place soon after the major tsunami (Tappin et al., 2008). Large

SMF can indeed generate tsunamis more disastrous than tsunamis generated by vertical uplift of sea-bottom mass of similar volume triggered by tectonic activity, known as earthquake-generated tsunami. Such SMF has been demonstrated as the origin of the 1998 PNG tsunami that generated run-up heights of 10 m over a stretch of 20 km along the coastline. The slide involved a relatively small volume of 4 km^3, located some 20 km offshore and at a water depth of 550 m, sliding over a distance of 5 km. This sea-bottom motion of the SMF generated the tsunami waves. A two-dimensional (2D) depth-averaged shallow water (SW) simulation model was successfully used to reproduce the distribution of observed run-up heights (Heinrich et al., 2001). The SW approximation is now frequently adopted for simulating the SMF motion and the associated water wave propagations. This type of 2D depth-averaged SW approximation is therefore used in this thesis for simulating SMF-generated tsunami and its subsequent propagation through the deep ocean, leading to the ultimate run-up along the beaches.

2.2.3 SMF Tsunamis in the Northern South China Sea

In November 1991, a SMF occurred during the preliminary pile sinking process in the crude oil terminal project of China Sinopec at Aoshan, Xingzhong. This landslide caused the collapse of many pile foundations and generated a 2 m to 3 m tsunami (Yongfu and Bolin, 2014). Geological surveys have discovered a wide range of past SMFs at the outer continental shelf and the upper continental slope of Northern South China Sea (NSCS), at the depth of about 180 m to 650 m. The SMF landslides in NSCS are related to hydrocarbon formation of gas hydrates, which are ice-like compounds mainly consisting of methane and water. The impact of accumulated high pore pressure and water precipitation resulting from natural gas

hydrate decomposition, working alone or in conjunction with earthquake, are capable of triggering SMFs.

Recent research related to oil and gas exploration and development in China, for example, also reveals significant potential tsunami risks arising from SMF. With mature and ongoing development of hydrocarbon, the NSCS is a hot spot for oil and gas exploration and production. The Baiyun Depression in this area has been observed to have suffered eleven SMF landslides of different scales in the past. The generation, propagation and run-up of tsunamis within 4.5 hours travel time generated by the Landslide S4 in a sea area of 672 km × 673 km were simulated by using the GEO-WAVE Boussinesq model (Yongfu and Bolin, 2014). The simulation results indicated that Landslide S4 may generate a tsunami with the maximum height of 17.5 m, occurring on the Dongsha Islands. Tsunami wave height along the coastal line is generally less than 1.5 m, but with 32 locations displaying exceptionally high run-ups. The maximum run-up at the continental coastal line is 5.3 m and the maximum inundation distance is 1600 m, occurring at the Shanwei City.

Dating back three centuries, numerous different historical records have alluded to a disastrous tsunami on the southwestern Taiwan coast sometime between 1781 and 1782, with a reported death toll of more than 40,000. Comparing the simulation results based upon 13 numerical models of tsunamis generated from different sources including earthquake, volcano, and SMF, Li et al. (2015) suggested that a seismically triggered SMF initiated on the upper portion of the continental slope offshore from southwestern Taiwan is the most likely source of the eighteenth

century mega tsunami event. From further survey of literature, it may be surmised that SMF-generated tsunamis were not uncommon in the past. This brief review has revealed the potential that many coastal areas in the region, including Sabah and Sarawak, are exposed to high vulnerability due to SMF-generated tsunami attacks.

2.2.4 SMF-Generated Tsunami Simulation Models

Using Non-Hydrostatic Wave (NHWAVE) model simulations, Ma et al. (2013) investigated the dependence of landslide motion and the associated tsunami wave generation on parameters such as sediment settling velocity, initial depth of the landslide and slide density. NHWAVE solves the non-hydrostatic Navier-Stokes equations in a domain over a surface and terrain in the 3D sigma-coordinate system by employing a finite volume scheme. The sigma-coordinate system allows the surface to correspond with model terrain, providing a better vertical resolution at the surface layer. Simulation results show that the slide motion and the water waves, which the motion generates, are both sensitive to these three parameters. Further, the wave energy is mostly concentrated in a narrow band of the dominant slide direction for the waves generated by rigid SMF landslides, while directional spreading is more significant for waves generated by deformable SMF landslides. At the early stage of SMF landslide, the deformable landslide has larger speed and higher acceleration, resulting in larger initial surface waves. On the other hand, as the rigid landslide continuously accelerates, it can gain higher velocity and bigger momentum, and hence can generate larger waves eventually.

Simple SMF tsunami models are often used for quick hazard assessment in the initial preliminary investigation. The model is commonly based on an empirical

formulation using simple geological and geometrical parameters to quickly predict reasonable tsunami vertical water displacement without having to run extensive computations. Watts (1998, 2000) conducted an experimental study of water waves generated by SMF to develop an empirical function for projecting wave displacement near the source generation. SMFs can be categorized as underwater slides and slumps, and the analysis of tsunami generated by slides and slumps may provide the approximate upper and lower bounds for tsunami vertical displacement to be expected in many situations (Grilli and Watts, 2005). Therefore, the empirical formulation proposed by Watts et al. (2003) is adopted in this thesis to generate the initial waves caused by the Brunei SMF Slide to simulate the worst-case scenario for hazard assessment.

2.3 The Great Eastern Japan Earthquake and Tsunami on 11 March 2011

For the 2011 GEJET event that killed 20,000 people, published models of tsunami propagation and coastal run-up under-predict the observed run-up heights measuring up to 40 m along the coast of the Sanriku district in the northeast part of Honshu Island. For example, Grilli et al. (2013) could not match this largest run-up height of 40 m measured along the Sanriku coast between 39.5°N and 40.25°N, even using the new co-seismic tsunami sources. Furthermore, simulations performed by MacInnes et al. (2013) using ten different earthquake sources could produce run-up heights within 20% difference from those measured, except for those in the Sanriku district. They were also unable to match the large run-up heights along a narrow beam measured at north of 39°N. The existence of an additional tsunami generation mechanism is therefore postulated to be the cause of this mismatch. While the primary source of the tsunami was the vertical

displacement of the seafloor lifted up by the earthquake, an additional tsunami source is also required to account for the unusually high and concentrated waves in the Sanriku district. The most likely additional tsunami source was postulated to be an SMF. Further slope stability analysis reveals that the horizontal acceleration from the earthquake itself was sufficiently large to trigger an SMF. Along the central Sanriku coast, the tsunami run-ups and inundations generated by the dual source consisting of an earthquake-tsunami plus an SMF-tsunami can indeed reproduce the field observations quite well, whereas the earthquake-seismic source alone severely under-predicts the field observations (Tappin et al., 2014). The conclusion that a significant part of the 2011 GEJET was generated by a SMF source has important implications for assessment of tsunami hazards in the Tohoku region as well as in other tectonically similar regions. This suggests a major, and insufficiently appreciated, tsunami hazard source exists due to SMF in this region, as well as in other tectonically similar regions. The need for new approaches to tsunami hazard estimation, the uncertainties regarding the past events, and the possibility of SMF-generated secondary tsunamis are challenges that must be addressed in future studies (Tappin et al., 2014).

2.4 Inundation Maps

To better prepare the coastal communities to be resilient to future potential tsunamis, it is necessary to understand the possible impacts of tsunami on coastal areas. As an essential part of tsunami early warning system, inundation maps are developed to understand coastal inundation and to assess tsunami hazards for highlighting areas that could be affected by a tsunami. The ability to visualize the inundated depth and the extent of inundation distance provides possible tools and

information for local communities and authorities to identify safe areas for evacuation. A tsunami inundation map is an important planning tool, not only for preparedness and mitigation efforts, but also for other planning purposes, such as urban and land use planning.

To develop a practical tsunami inundation map, a study domain consisting of local coastal topography and bathymetry data are necessary. Topography is defined as the land height of a location relative to a fixed datum, while bathymetry is defined as the water depth of a location relative to the fixed datum. This study domain serves as a computational domain for simulation models. As the impact of a tsunami is significantly influenced by the shape of coastline and by the accuracy of land height and coastal water depth, high-resolution topography and bathymetry data, with grid size of not more than 50 m, are often required to produce informative inundation maps (Walsh et al., 2009; 2014).

In order to learn from the past events, inundation maps are often produced by simulating the past tsunami events using validated and verified simulation models (Borrero et al., 2006; Mishra et al., 2014; Wijetunge, 2006). An overview of such simulation models used in previous tsunami hazard assessments is presented in the next section. Simulating future potential tsunami events to produce inundation maps is also very important for mitigating the tsunami impact and preparing the coastal community. Simulation model outputs are often produced in a raster format to facilitate the overlaying of simulated impact, in terms of inundated depth and inundation distances, on a base map using a geographic information system (GIS) software. This method is adopted in this thesis.

2.5 Tsunami Run-up and Inundation Models

MOST (Method of Splitting Tsunami), COMCOT (Cornell Multi-grid Coupled Tsunami), COULWAVE (Cornell University Long and Intermediate Wave Modeling Package), NHWAVE (Non-Hydrostatic Wave) and FVCOM (Finite Volume Coastal Ocean Model) are some of the well-known tsunami simulation models from the United States of America. Other equally well-known tsunami simulation models include TUNAMI-N2 (Tohoku University's Numerical Analysis Model for Investigation of Near-field tsunamis, No. 2) from Japan, ANUGA (Australian National University-Geoscience Australia) and Delft3D-FLOW from Netherlands. Table 2.1 summarizes the governing equation, numerical method and WD algorithm used in these models, as well as the key features and constraints.

As observed in Table 2.1, the NSWE is the widely used governing equation in most of the well-known tsunami simulation models. Generally, tsunami has a wavelength that is significantly larger than the water depth, thus fitting the assumption of long wave with the property that the vertical velocity is small enough to be considered negligible. This assumption is based on the derivation of the NSWE from the Euler's equations derived from mass conservation law (see Appendix A). As a tsunami wave propagates over a continental shelf and approaches a coastal region, where the water depth is shallow, the velocity of the tsunami is reduced and the wavelength is shortened, resulting in an increase in wave height of the tsunami wave. The NSWE including bottom friction is well suited for modelling such hydrodynamics in shallow coastal region, with no wave breaking.

Table 2.1: Summary of the reviewed tsunami run-up and inundation models

Model	Governing equation	Numerical method	WD algorithm	Key feature/ constraint
MOST	NSWE	FD	Element removal	• For non-breaking wave • Steep fronts may cause instability • Bathymetry correction tool
COMCOT	NSWE	FD	Element removal	• For non-breaking wave • Steep fronts may cause instability
COULWAVE	Boussinesq	FD/FV	Depth extrapolation	• For breaking/non-breaking wave • Suitable for dam break problem
NHWAVE	Navier-Stokes	FV	Element removal	• For breaking/non-breaking wave • Non-hydrostatic
FVCOM	NSWE	FV	Thin film	• For breaking/non-breaking wave • Suitable for dam break problem
TUNAMI-N2	NSWE	FD	Element removal	• For non-breaking wave • Steep fronts may cause instability
ANUGA	NSWE	FV	Element removal	• For non-breaking wave • Suitable for dam break problem
Delft3D-FLOW	NSWE	FD	Element removal	• For breaking/non-breaking wave • Suitable for dam break problem

Some models, such as COULWAVE, employ the Boussinesq equations that include additional dispersion terms to properly model dispersive waves. However, the range of applicability of Boussinesq equations are not significantly greater than that of